FLOW CYTOMETRIC MEASUREMENT OF FLUORESCENCE RESONANCE ENERGY TRANSFER ON CELL SURFACES

Quantitative Evaluation of the Transfer Efficiency on a Cell-by-Cell Basis

L. TRÓN, J. SZÖLLŐSI, AND S. DAMJANOVICH
Department of Biophysics, Medical University School of Debrecen, H-4012 Debrecen, Hungary

S. H. HELLIWELL, D. J. ARNDT-JOVIN, AND T. M. JOVIN
Department of Molecular Biology, Max Planck Institut für Biophysikalische Chemie, D-3400 Göttingen, Federal Republic of Germany

ABSTRACT A method has been developed for the determination of the efficiency (E) of the fluorescence resonance energy transfer between moieties on cell surfaces by use of a computer-controlled flow cytometer capable of dual wavelength excitation. The absolute value of E may be calculated on a single-cell basis. The analysis requires the measurement of samples stained with donor and acceptor conjugated ligands alone as well as together. In model experiments HK 22 murine lymphoma cells labeled with fluorescein-conjugated concanavalin A (Con A) and/or rhodamine conjugated Con A were used to determine energy transfer histograms. Using the analytic solution to energy transfer in two dimensions, a high surface density of Con A binding sites was found that suggests that the Con A receptor sites on the cell surface are to a degree preclustered. We call this technique flow cytometric energy transfer (FCET).

INTRODUCTION

Measurements of fluorescence energy transfer have been applied to a wide range of problems in molecular biology (1). This technique has been exploited to obtain both static and dynamic information about intramolecular (2–4) and intermolecular (5–9) distance relationships.

In systems with donor and acceptor fluorophores located at well-defined sites, the interpretation of the energy-transfer efficiency is straightforward. In molecular systems with a random distribution of donors and/or acceptors, the measured energy transfer efficiency represents an averaged value over the different individual donor-acceptor orientations and stoichiometry (10, 11). A somewhat similar situation is faced in the case of even more complicated systems where donors and/or acceptors are distributed in lipid vesicles or cell membranes (7, 12–14). Some of these systems may be better treated by theories of energy transfer in two dimensions where donors and acceptors are distributed on a surface (15–19).

Resonance energy transfer between specific sites on the cytoplasmic membrane of mammalian cells has been investigated experimentally in cell suspensions with a steady-state fluorimeter (20) and on a single-cell basis with a microscope (21) and a flow cytometer (22–24). Energy transfer data determined with the first method are averaged values over the entire homogeneous or heterogeneous population. The use of flow methods, however, makes possible the detection of energy transfer on a cell-by-cell basis, thus viewing subpopulations separately. In spite of this great advantage, the flow methods have been used previously to give only relative energy transfer efficiency rather than an absolute value.

In the present study, we describe a method for the direct determination of the efficiency of the energy transfer on individual cells. The method allows one to investigate the cross correlation of energy transfer efficiency to other experimental parameters in a heterogeneous cell population or to enable sorting of cells by gating with respect to preset transfer efficiency values.

In this study, fluorescein isothiocyanate- (FITC-) conjugated concanavalin A (Con A) and tetramethyl rhodamine isothiocyanate- (TRITC-) conjugated Con A were used as a donor-acceptor pair, but other ligands and donor-acceptor dye pairs may be used as well.

MATERIALS AND METHODS

Cells

HK 22 [(C3HxDBA/2)f1] murine lymphoma cells with the H-2K^k haplotype (25) (the kind gift of Dr. Bodo Holtkamp, Cologne, Federal

Reprint requests should be sent to the Department of Molecular Biology, Max Planck Institute für Biophysikalische Chemie, D-3400 Göttingen, Federal Republic of Germany.

Republic of Germany) were grown in Dulbecco's minimal essential medium containing 10% fetal calf serum (FCS) and antibiotics (Line HK22, previously named T41).

Ligand Labeling

FITC and TRITC were purchased from Molecular Probes (Junction City, OR) and from Baltimore Biological Laboratory, (Cockeysville, MD), respectively. Jack bean concanavalin A tetramer (Con A) was obtained from SERVA Feinbiochemica Gmbh & Co. (Heidelberg, Federal Republic of Germany). The procedure used for the lectin labeling was the same as previously described (22). The extinction coefficients of FITC (495 nm) and of RITC (553 nm) are $6.3 \times 10^4\ M^{-1}\ cm^{-1}$ (26) and $3.4 \times 10^4\ M^{-1}\ cm^{-1}$ (22), respectively. The average labeling ratios (fluorophore/Con A tetramer) were 2.2 for fluorescein, and 2.6 for rhodamine.

Labeling of the Cells with FITC-ConA and TRITC-ConA

Cells were collected from medium and washed twice with phosphate buffered saline (PBS). Cells (6×10^6 cells/ml in PBS) were incubated in the presence of 0.2 mg/ml total lectin concentration at 4°C in 0.2 ml volume with gentle agitation every 5 min. After 30 min cells were washed by centrifugation through a layer of 3 ml 50% FCS onto a cushion of Lymphoprep (see procedure described in reference 22) to avoid aggregation of cells. Cells were fixed in 1% formaldehyde and analyzed in the flow cytometer.

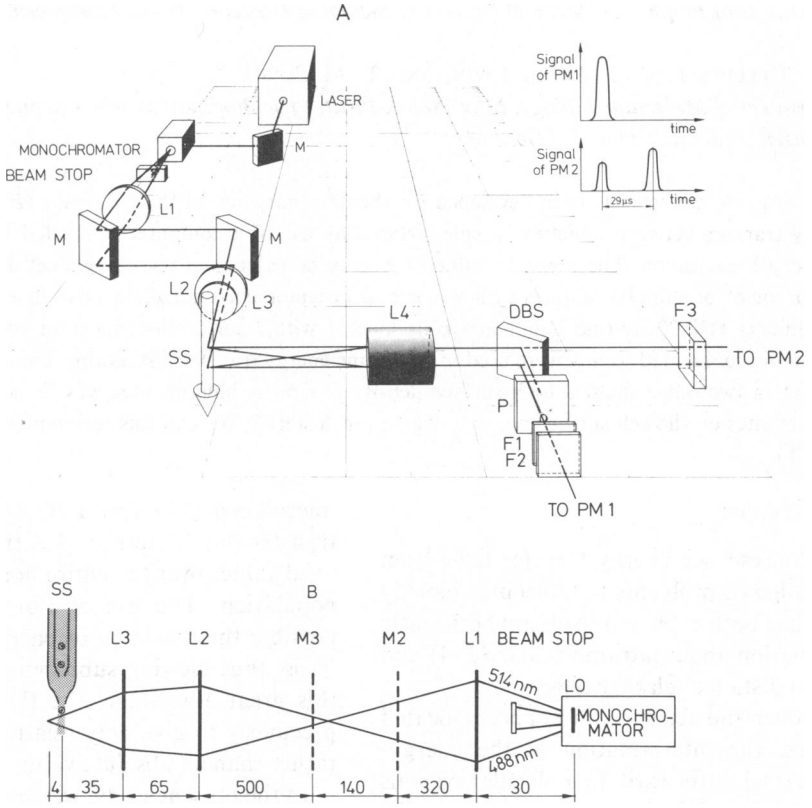

FIGURE 1 The optical arrangement of the flow cytometer. The components were as follows. The *laser* was a 15-W CW argon ion laser (Spectra Physics model 171); the *monochromator* was an Anaspec 300S containing a prism as a dispersive element; *L0*, output lens of the *monochromator; L1*, ϕ = 17 mm, f = 200 mm biconvex spherical lens; *L2*, ϕ = 17 mm, f = 285 mm cylindrical lens; *L3*, ϕ = 17 mm, f = 40 mm achromatic spherical lens; *L4*, f = 14 mm condensor. *M1* and *M2* were front surface plane laser reflectors (Spectra Physics, USA; Cat. No. G0050-003); *M3* was a 20Z20 ER.1 plane reflector (Newport Corporation, USA); *Beam stop;* brass strip; *SS*, sample stream; *DBS*, dichroic beam splitter FT 580 (Zeiss, F.R.G.); *P*, pinhole (ϕ = 1 mm) in the *beam stop* unit; *F1*, 3-mm-thick band-pass filter centered at 535 nm FWHM-36 nm (Biophysics Europa, Bensheim, F.R.G.); *F2*, 1-mm-thick high-pass filter OG 530 (Schott, Mainz, F.R.G.); *F3*, 1-mm-thick high-pass filter OG 590 (Schott); *PM1*, EMI 9558; *PM2*, EMI 9658A; *PM3* (not shown in the diagram), EMI 9558QB. (*A*) The optical arrangement in perspective. The 488 and 514 nm laser lines were focused on the sample stream carrying a suspension of cells labeled with fluorescent dye conjugated ligands. All other laser lines were blocked out with a *beam stop*. Excitation of the fluorophores of the same cell at the selected wavelengths was separated both temporally and spatially. The emission excited at 488 nm was detected in both detection channels (see text), but that excited at 514 nm was detected only with *PM2*. The latter emission was blocked reaching *PM1* with a *beam-stop-pinhole* unit. The signal detected by *PM1* was coincident in time with the first one detected with *PM2*. The second signal of *PM2* (due to excitation at 514 nm) was delayed relative to signals from 488 nm excitation. The light scattered in the forward direction was detected by *PM3* (not shown in the figure) via a fiber optic element tilted at 7° relative to the excitation laser beam axis. The fiber-optic element collected light scattered between 5° and 10°. *PM3* was preceeded by a 9-mm-thick 488-nm line-pass filter (Corion, USA). (*B*) Vertical section of the input optics along the optical axis. The measures are given in millimeters. The 488 nm and 514 nm excitation lines are in the same vertical plane separated by 10 mm at *L1* and 7 mm at *L3*, intersecting each other just before *M3* and 4 mm behind the *SS*. The intersection of the 488-nm beam with the sample stream was 0.5 mm below the double nozzle orifice (50 μm diam) and 0.6 mm above the 514 nm beam-*SS* intersection. The beam profile at SS is elliptical with a horizontal long axis = 40 μm and short axis = 20 μm.

Instrumentation

A 15-W argon ion laser (Spectra-Physics Inc., Mountain View, CA, model 171) was used in the all-lines mode throughout the experiments. The laser beam was directed by a mirror into an Anaspec (Anaspec Research Laboratory, Newbury, England) 300S laser monochromator (Fig. 1). By use of a beam stop the 488 and 514 nm lines were selected from the lines dispersed by the monochromator in a vertical plane. The spatially separated 488 and 514 nm beams were focused onto the sample stream by three lenses and two additional mirrors (Fig. 1), resulting in excitation of the fluorophores of the same cell at two wavelengths displaced in time. The experimental arrangement was a modified version of the one described in (27).

The fluorescence arising from the cells was detected with two photomultiplier (PM) tubes using a condenser, a dichroic beam splitter, and appropriate optical filters. PM1 detected the emitted light through use of a 535 nm band-pass and an OG 530 cutoff filter. PM2 detected fluorescence beyond 590 nm (580 nm dichroic filter and OG 590 cutoff filter). In some cases the latter filter was replaced by an OG 570 or an OG 610 filter (see Results and Discussion). PM1 detected emission arising exclusively from 488-nm excitation (I_1 signal), since the emission arising from 514-nm excitation was blocked with a beam stop. PM2, however, detected emission arising from excitation at both 488 (I_2 signal) and 514 nm (I_3 signal). The forward small-angle light scattering was collected by fiber optics and measured with PM3 (not shown). Detection of signals by PM1 and PM2 was gated with light-scattering signals of appropriate amplitudes. Data (pulse heights and pulse areas) belonging to individual cells were collected and stored in a correlated form by a PDP 11/45 computer (Digital Equipment Corp., Marlboro, MA).

In the experimental arrangement depicted in Fig. 1 there were two detection channels: the first and second detection channel referred to all optical and electronic components associated with PM1 and PM2, respectively. Three fluorescence signals (I_1, I_2, and I_3) could be measured from a single cell in these two detection channels.

Determination of Energy Transfer Efficiency

Three fluorescence signals were measured from each cell with the optical arrangement and detection system described in the previous section. Signals from cells labeled with only the donor or the acceptor were measured to obtain the correction parameters used in Eqs. 1–3 below. The signals from cells labeled with both fluorophores were then corrected to give the transfer efficiency. These parameters were corrected for spectral overlapping and differences in the excitability and detectability of the donor and acceptor, and could be defined as follows: $S_1 = I_2/I_1$, determined using cells labeled only with the donor; $S_2 = I_2/I_3$, determined using cells labeled only with the acceptor; $S_3 = I_3/I_1$, determined using cells labeled only with the donor. The relationships between the detected intensities and the relative detection efficiencies for the various signals arising from the donor and the acceptor chromophores are summarized in Table I.

Consider a cell labeled with both FITC (donor) and TRITC (acceptor) conjugated ligands. In the absence of energy transfer we denote the theoretical, unperturbed, directly excited fluorescence intensity of fluorescein (excited at 488 nm, measured at 535 nm) as I_F and that of rhodamine with excitation at 514 nm and emission >590 nm as I_R. We denote the energy transfer efficiency by E. With these parameters as well as S_1, S_2, S_3, as defined above, the three measured fluorescence intensities from a doubly labeled cell are

$$I_1(488, 535) = I_F(1 - E) \quad (1)$$

$$I_2(488, >590) = I_F(1 - E)S_1 + I_R S_2 + I_F E\alpha \quad (2)$$

$$I_3(514, >590) = I_F(1 - E)S_3 + I_R + S_3/S_1 \cdot I_F E\alpha. \quad (3)$$

I_1 is $<I_F$ by an amount that is lost due to the energy transfer. The measured signal, I_2, has three additive terms: (*a*) the fraction of the quenched fluorescein emission overlapping the second detection channel, (*b*) the directly excited (at 488 nm) rhodamine fluorescence, and (*c*) the sensitized emission of rhodamine due to the energy transfer. This last term is proportional to the fractional decrease in the intensity of fluorescein (excited at 488 nm, detected at 535 nm) due to the energy transfer. The proportionality factor is α, which is the ratio of the fluorescence intensity of a given number of excited rhodamine molecules measured with 488 nm excitation and >590 nm emission to the fluorescence intensity of the same number of excited fluorescein molecules measured with 488 nm excitation and 535 nm emission. This is a constant for a given experimental arrangement and a particular pair of donor and acceptor conjugated ligands and must be measured for every defined case. The intensity I_3 is the sum of (*a*) the fraction of the quenched fluorescein emission (excited at 514 nm) that overlaps the rhodamine detection channel, (*b*) the rhodamine fluorescence coming from the direct excitation (514 nm), and (*c*) the sensitized emission of rhodamine due to the energy transfer. The ratio of S_3 to S_1 corrects for the fact that fewer fluorescein molecules are excited at 514 nm than at 488 nm. From Eqs. 1–3, Eq. 4 can be derived:

$$\frac{E}{1 - E} = \frac{1}{\alpha}\left[\frac{(I_2 - S_2 I_3)}{\left(1 - \frac{S_3}{S_1}S_2\right)I_1} - S_1\right]. \quad (4)$$

Because all of the parameters on the right side of Eq. 4 can be experimentally determined, we denote the right side of Eq. 4 as A and solve for the energy transfer efficiency E (as well as I_F and I_R):

$$E = A/(1 + A). \quad (5)$$

In the experiments described in this paper, cellular autofluorescence contributed <2% to I_1, I_2, and I_3. Under conditions in which the contribution was appreciable, a more complicated expression for Eq. 4 was necessary to take into account the spectral characteristics of the autofluorescence. We are exploring experimental designs that permit an independent assessment of autofluorescence on a cell-by-cell basis.

TABLE I
EMISSION SIGNALS AND RELATIVE DETECTION EFFICIENCIES

Emitting species	Signals	Detection efficiencies		
		I_1	I_2	I_3
	nm			
	λ_{em}	535 ± 18	>590	>590
	λ_{exc}	488	488	514
F (direct excitation)		1	S_1	S_3
R (direct excitation)		0	S_2	1
$F \rightarrow R$ (sensitized emission)		0	α	$\alpha S_3/S_1$

F and R refer to the fluorescein and rhodamine chromophores, respectively, S_1, S_2, S_3, and α are defined in the text. In the case of the sensitized emission, the donor-acceptor spectral interconversion is integrated into the definition of detection efficiency.

Determination of α

The fluorescence of fluorescein from a cell measured in the first detection channel may be written as

$$[B_F L_F \phi_{F\lambda} \rho_\lambda t]\,[Q_F \gamma_F \xi_F] = N_F C_F \quad (6)$$

where B_F is the number of binding sites occupied by FITC conjugated ligands, L_F is the fluorophore to ligand labeling ratio for the FITC conjugated ligand; $\phi_{F\lambda}$ is the absorption cross section of a fluorescein molecule at the excitation wavelength λ (in square centimeters); ρ_λ is the irradiance of the excitation beam, divided by the energy of the photons

(photons per square centimeter per second); t is the equivalent time a cell resides in the radiation field of ρ_λ density (in seconds); Q_F is the fluorescence quantum efficiency of fluorescein; γ_F is the fraction of the total fluorescein emission reaching the phototube in the first detection channel; and ξ_F is the average voltage on the output of the detectors per photon reaching the phototube. This factor includes the detection efficiency of the phototube for the fluorescein emission in the first detection channel and the gain of the phototube (in millivolts per photon). Subscript F refers to fluorescein.

In the above expression, the product of the first five factors yields N_F, the number of the excited fluorescein molecules. Let C_F denote the product of the last three terms, which contain only the spectral characteristics of the fluorophore and instrumental parameters. This factor gives the ratio of the fluorescence signal measured in the first detection channel to the number of the excited fluorescein chromophores.

A similar expression may be written for the fluorescence signal measured in the second detection channel from a cell labeled with TRITC conjugated ligand:

$$[B_R L_R \phi_{R\lambda} \rho_\lambda t]\,[Q_R \lambda_R \xi_R] = N_R C_R \tag{7}$$

where R refers to rhodamine.

Let M_F and M_R denote the mean value of the fluorescence frequency distribution of I_1 and I_2 from two separate populations of cells saturated either with FITC conjugated ligands or TRITC conjugated ligands, respectively:

$$M_F = \bar{B}_F L_F \phi_{F\lambda} \rho_\lambda t C_F \tag{8}$$

$$M_R = \bar{B}_R L_R \phi_{R\lambda} \rho_\lambda t C_R \tag{9}$$

where $\bar{B}_F$ and $\bar{B}_R$ are values averaged over the analyzed populations.

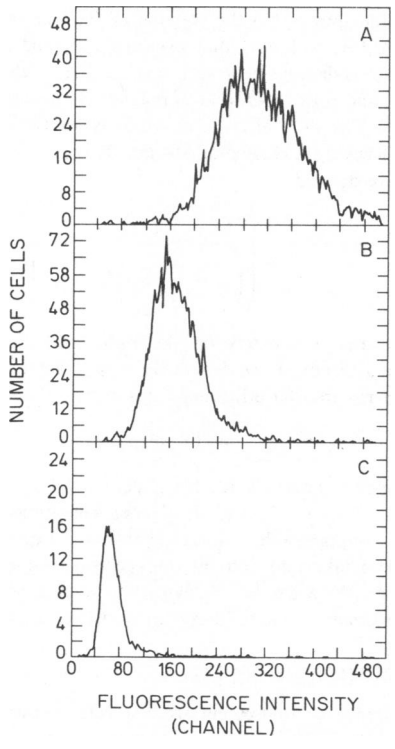

FIGURE 2 Frequency distribution histograms of fluorescence signals of HK 22 cells labeled with FITC-ConA. (*A*) Fluorescence excited at 488 nm and detected by *PM1* (I_1); (*B*) Fluorescence excited at 488 nm and detected by *PM2* (I_2); (*C*) Fluorescence excited at 514 nm and detected by *PM2* (I_3). The three distributions were measured without altering any of the set parameters. Cells were labeled as described in Materials and Methods.

The fluorescence of a doubly labeled cell measured at 488 nm excitation and 535 nm emission was decreased by an amount of $I_F E$ because energy was transferred to the rhodamine. $I_F E$ is equivalent to the emission from $I_F E/C_F$ excited fluorescein chromophores detected at 488 nm excitation and 535 nm emission. Due to this energy transfer $I_F E/C_F$ rhodamine molecules become excited. The transferred energy is detected as rhodamine fluorescence with an intensity of $(I_F E)(C_R/C_F) = I_F E\,\alpha$ in the second detection channel. Expressing the ratio C_R/C_F in terms of Eqs. 8 and 9 we derive

$$\alpha = \frac{M_R \bar{B}_F L_F \epsilon_{F\lambda} \rho_\lambda}{M_F \bar{B}_R L_R \epsilon_{R\lambda} \rho_\lambda} \tag{10}$$

where ϵ is the molar absorption coefficient.

Error Estimations

It is important to distinguish the relative contributions to the observed distributions of A and E arising from instrumental measurement uncertainties and true biological variation. A first-order error propagation analysis of Eqs. 4 and 5 yield the following expressions for the variances σ^2 corresponding to the calculated values of A and E in terms of those measured or estimated for the parameters and signals S_1, S_2, S_3, I_1, I_2, I_3, and α. Not included are the possible influences of autofluorescence:

$$\sigma_A^2 \simeq \left(\frac{A}{\alpha}\right)^2 \sigma_\alpha^2 + \frac{1}{\left(1 - \dfrac{S_2 S_3}{S_1}\right)^2} \left\{ \left(\frac{S_2 S_3}{S_1^2} A + \frac{1}{\alpha}\right)^2 \sigma_{S_1}^2 + \left[\frac{S_3}{S_1} A + \frac{\left(S_3 - \dfrac{I_3}{I_1}\right)}{\alpha}\right]^2 \sigma_{S_2}^2 + S_2^2 \left(\frac{A}{S_1} + \frac{1}{\alpha}\right)^2 \sigma_{S_3}^2 + \frac{1}{(\alpha I_1)^2} \left[\frac{(I_2 - S_2 I_3)^2}{I_1^2} \sigma_{I_1}^2 + \sigma_{I_2}^2 + S_2^2 \sigma_{I_3}^2\right] \right\} \tag{11}$$

$$\sigma_E^2 \simeq \frac{1}{(1 + A)^4} \sigma_A^2 . \tag{12}$$

RESULTS AND DISCUSSION

In the experiments discussed below, cells labeled with FITC-Con A and/or TRITC-Con A were used to demonstrate the applicability of this calculation method for determination of energy transfer efficiency on a cell-by-cell basis. The frequency distributions of the signals for cells labeled only with fluorescein or rhodamine conjugated Con A are displayed in Figs. 2 and 3. Instrumental factors were kept constant for the experiments. For cells labeled with fluorescein-conjugated ligand alone, the intensity of the emission at 535 nm with excitation at 488 nm is defined as I_1 (Table I). The corresponding intensity I_2 is proportional to I_1 by the factor S_1 (Fig. 4 *A*) and the intensity I_3 is proportional to I_1 by the factor S_3 (Fig. 4 *B*). Similarly the signals from cells labeled with rhodamine-conjugated ligands alone are linearly related. Thus, I_2 is proportional to I_3 by a factor S_2 (Fig. 4 *C*). In this case, I_1 corresponds to the background cellular emission that is negligible in magnitude. The S_1, S_2, and S_3 correction factors can also be determined from the frequency distributions of the ratios of signal intensities (I_2/I_1, I_3/I_1, I_2/I_3) derived from singly labeled cells.

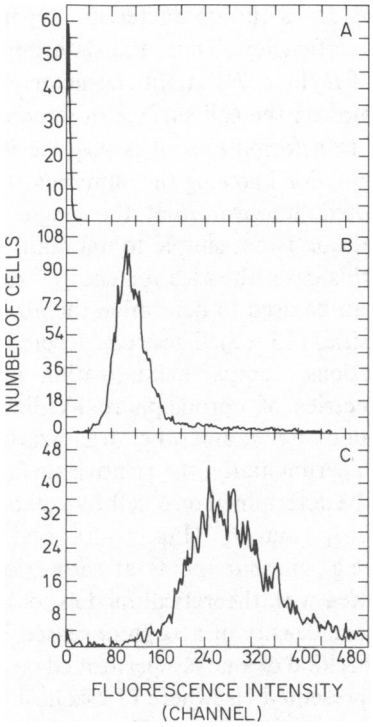

FIGURE 3 Frequency distribution histograms of fluorescence signals of HK 22 cells labeled with TRITC-ConA. *A*, *B*, and *C* refer to the same conditions described in the legend to Fig. 2.

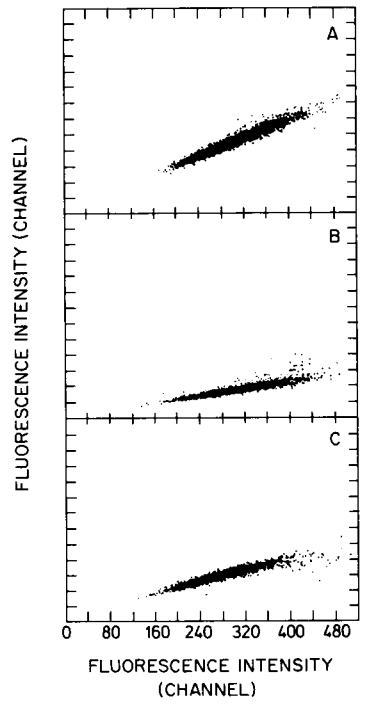

FIGURE 4 Correlation of fluorescence signals from cells labeled with only FITC-ConA or TRITC-ConA. *A* and *B*, scattergrams of cells labeled with FITC-ConA. *A*, *y*-axis signals measured at 488 nm excitation and >590 nm emission (I_2), *x*-axis signals measured at 488 nm excitation and 535 ± 18 nm emission (I_1), slope is S_1. *B*, *y*-axis signals measured at 514 nm excitation and >590 nm emission (I_3); *x*-axis I_1 signals, slope is S_3. *C*, scattergram of cells labeled with TRITC-ConA, *y*-axis I_2 signals, *x*-axis I_3 signals, slope is S_2.

The determination of α according to Eq. 10 involves the estimation of the mean values for the fluorescence intensities I_1 and I_2 of two samples of cells saturated with either FITC or TRITC conjugated ligands, respectively. It requires the determination of the fluorophore-to-ligand labeling ratio for both the FITC- and TRITC-conjugated ligands, as well as the molar absorption coefficients for both types of ligands at the excitation wavelengths used for the evaluation of M_F and M_R. It is advantageous to measure the distributions for the determination of M_F and M_R at the same excitation wavelength (e.g., at 488 nm) unless it results in values close to the background. In the case of low signal-to-noise ratios, the determination of the distribution for M_R has to be accomplished in the second detection channel with 514 nm excitation and that for M_F in the first detection channel with 488 nm excitation. This requires knowledge of the molar absorption coefficient of the fluorophore at 514 nm (ϵ_R) and the relative quantum density of the two excitation beams.

The above treatment is valid for the case in which donor and acceptor fluorophores are bound to the same type of ligand. Under these circumstances the number of the available binding sites is the same, so the term $\bar{B}_F/\bar{B}_R$ cancels in Eq. 10 for α. If the donor and acceptor labeled ligands are different (e.g., TRITC-Con A and FITC-anti-H2 antibody), one can no longer assume the equality of $\bar{B}_F$ and $\bar{B}_R$ and their ratio must be determined.

Obtaining a constant value of E with different optical filters in the first and the second detection channel is a simple check of the procedure. Upon altering the optical characteristics of the F3 filter (Fig. 1), the proportionality factors (S_1–S_3) and the numerical value of the α parameter changes. These alterations, however, should not affect the absolute value of the fluorescence energy transfer efficiency. In Table II we list the mean values of the transfer efficiency distributions for a number of different doubly

TABLE II
INDEPENDENCE OF THE FLUORESCENCE ENERGY TRANSFER EFFICIENCY ON EMISSION SPECTRAL REGION

$\frac{[R]\text{-Con A}}{[F]\text{-Con A}}$	Energy transfer efficiency		
	A	*B*	*C*
	%	%	%
0.20	6.0	5.2	6.0
0.29	8.5	7.3	8.5
0.60	14	15	13
1.25	19	18	20
2.54	23	25	24
5.29	27	26	28
8.47	28	28	30

[R]-Con A/[F]-Con A is the rhodamine to fluorescein ratio during the labeling of the cells with the fluorescent ligands. The total ConA concentration was kept constant (0.2 mg/ml). The measurements were carried out using different cutoff filters in the second detection channel: (*A*) OG 570, (*B*) OG 590, (*C*) OG 610.

labeled samples analyzed successively using three different cutoff filters in the second detection channel. Good overall agreement was observed between the three energy-transfer efficiency values calculated for each of the seven samples.

After the determination of correction factors we can easily generate the energy transfer histograms of HK 22 cells labeled with both FITC-Con A and TRITC-Con A (Fig. 5). The energy transfer values increased together with the relative concentration of the acceptor TRITC-Con A (the total concentration of Con A was maintained at saturation levels). The HK 22 cells seemed to be homogeneous according to the energy transfer distribution curves indicating that there were no significant differences in the surface density of the ConA binding sites on different cells.

The standard deviation of E is a function of both instrumental and biological variation. A detailed investigation of their respective contribution has been treated in another publication (28). For a system similar to the one described in this paper, the propagation of instrumental error contributes 4.6% to the measured coefficient of variation E (11.9%), leaving $CV_{E,\text{biol}} = 7.3\%$.

In addition to the energy transfer histograms, the frequency distribution of $A = E/(1 - E)$ is of interest, since for a single donor–single acceptor system $E/(1 - E) = (R_0/R)^6$, where R is the distance between donor and acceptor, and R_0 is the characteristic separation giving 50% transfer efficiency. Thus, the determination of the distribution of $E/(1 - E)$ might characterize the proximity relationships on the cell surface in a more direct way. With simple transformations, it is possible to calculate a distance distribution knowing the numerical value of R_0. It has to be noted, however, that the single donor–single acceptor condition is not simple to maintain with cellular samples. In this case, theories for energy transfer in two dimensions can be used to determine the absolute surface acceptor densities (15–19). These can accomodate nonrandom distributions, compartmentalization into domains, various geometries of chromophore localization on the macromolecular carrier, and other organizational features of interest. Experimentally, the relative surface density of acceptor can be determined on a cell-by-cell basis from the quantities E, I_F, and I_R (Eqs. 1–5), and appropriate calibrations, e.g., measurements at saturation. The data can be evaluated with theoretical models to determine the absolute surface density of acceptors sensed by the donor molecules. This kind of analysis performed on a cell-by-cell basis will be presented elsewhere (J. Szöllősi, LiTrón, and T.M. Jovin, in preparation). We applied the analytic solution to the energy transfer in two dimensions (18) to our data shown in Table II. The relative surface density of TRITC-ConA was calculated from the TRITC to FITC molar ratios using the known labeling ratios of conjugates and the fact that the ConA concentration was kept constant at saturation level. These relative surface densities and the corresponding mean values of energy transfer efficiencies were fitted with the theoretical curves, yielding an absolute surface density of $1.1 \times 10^4/\mu^2$ for ConA binding sites and a distance of closest approach between ConA molecules of 6 nm. A value for the critical transfer distance R_0 of 6 nm was used in these calculations (see also 22, 23). However, a simplified model of the cell surface corresponding to a smooth 15 μm sphere leads to a calculated surface density of $6.3 \times 10^3/\mu^2$ (from 4.4×10^6 Con A binding sites per cell; our determination). This value might be even much lower if the cell surface is irregular with a much larger area than assumed for the sphere. These data suggest that the Con A binding sites could be, to a degree, clustered on the cell surface, a result expected from to multiple sites of glycosylation of glycoproteins and glycolipids. This finding is in accordance with our previous studies (22, 23). The 6-nm minimal distance between bound Con A molecules is in good agreement with the crystallographic dimensions of 6.3 nm × 8.7 nm × 9 nm (29, 30).

The method presented here (FCET) offers the following advantages in comparison to steady-state energy transfer measurements using cell suspensions. (*a*) The intrinsic features of flow systems can be fully exploited: high sensitivity, high precision, multiparameter sensing, freedom from bleaching, scattering, and background artifacts, and sorting capability. (*b*) There is no necessity to elimi-

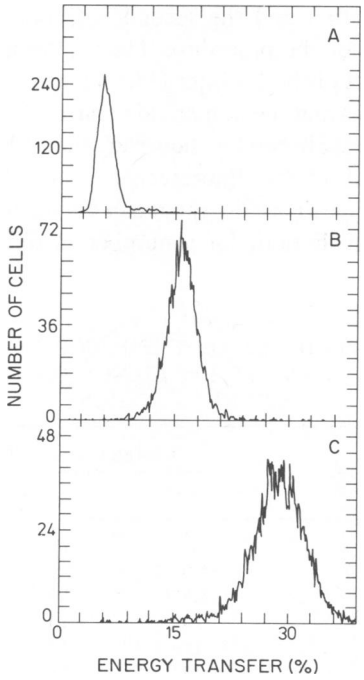

FIGURE 5 Frequency distribution histograms of the average fluorescence energy transfer efficiency between FITC-ConA and TRITC-ConA on HK 22 cells. Rhodamine to fluorescein ratios (*A*) 0.21; (*B*) 1.0; (*C*) 4.6. The total concentration of Con A was kept at a saturating level (0.2 mg/ml). The measured standard deviations corresponding to the mean values were 1.1, 2.3, and 4.4%; an estimate from Eqs. 11 and 12 of 3.4% was obtained for the intermediate case.

nate free ligands from the environment of the cell because the signals consist of pulses emanating from individual cells within a minute illuminated volume (5–50 pl). Thus, measurements can be carried out without separation procedures that might perturb a dynamic receptor-ligand equilibrium. (*c*) It is easy to restrict the analysis to undamaged cells by gating the data collection with light scattering signals of appropriate amplitudes, thereby suppressing contributions from dead cells or debris. (*d*) Interference from light scatter, a severe problem in steady-state fluorimetric determinations at high cell concentrations, is absent. (*e*) Rapid population analyses yielding frequency distributions of intensities of any derived quantity such as E are obtained. Thus, the homogeneity of the population can be assessed. In addition, correlations between the energy transfer values and other cellular parameters (e.g., size, position in the cell cycle, functional state, etc.) can be made. (*f*) Given the appropriate electronic and computational capabilities of the flow system, cellular subpopulations can be sorted according to the energy transfer property alone or in combination with other cellular features.

FCET is also being applied in our laboratories to other biological systems of interest, for example the surface organization of the major histocompatibility antigens (31) and polypeptide hormone receptors. In such cases, the technique offers an independent assessment of the dynamic properties of cell surface constituents to that provided by time-resolved spectroscopic measurements (32). Intracellular phenomena can also be explored (33).

We thank Dr. R. M. Clegg and Dr. E. D. Matayoshi for their helpful discussion, and Ms Annette von Bogen for assisting with tissue culture.

This work was carried out as a part of a research program between the Department of Molecular Biology, Max Planck Institut für Biophysikalische Chemie, Göttingen, FRG, and the Department of Biophysics, Medical University School of Debrecen, Debrecen, Hungary, jointly sponsored by the Deutsche Forschungsgemeinschaft and the Hungarian Academy of Sciences.

Received for publication 13 January 1983 and in revised form 11 June 1983.

REFERENCES

1. Stryer, L. 1978. Fluorescence energy transfer as a spectroscopic ruler. *Annu. Rev. Biochem.* 47:819–846.
2. Hahn, L.-H. E., and G. G. Hammes. 1978. Structural mapping of aspartate transcarbamoylase by fluorescence energy-transfer measurements: determination of the distance between catalytic sites of different subunits. *Biochemistry* 17:2423–2429.
3. Zukin, R. S., P. R. Hartig, and D. E. Koshland, Jr. 1977. Use of a distant reporter group as evidence for a conformational change in a sensory receptor. *Proc. Natl. Acad. Sci. USA.* 74:1932–1936.
4. Luedtke, R., C. H. Owen, J. M. Vanderkooi, and F. Karush. 1981. Proximity relationship within the Fc segment of rabbit immunoglobulin G analyzed by *p*-resonance energy transfer. *Biochemistry.* 20:2927–2936.
5. Epe, B., P. Woolley, K. G. Steinhauser, and J. Littlechild. 1982. Distance measurement by energy transfer: the 3′ end of 16-S RNA and proteins S4 and S17 of the ribosome of *Escherichia coli*. *Eur. J. Biochem.* 129:211–219.
6. Damjanovich, S., W. Bahr, and T. M. Jovin. 1977. The functional and fluorescence properties of *Escherichia coli* polymerase reacted with fluorescamine. *Eur. J. Biochem.* 72:559–569.
7. Stryer, L., D. D. Thomas, and C. F. Meares. 1982. Diffusion-enhanced fluorescence energy transfer. *Annu. Rev. Biophys. Bioeng.* 11:203–222.
8. Lobb, R. R., and D. S. Auld. 1980. Stopped-flow radiationless energy transfer kinetics: direct observation of enzyme-substrate complexes at steady state. *Biochemistry.* 19:5297–5302.
9. Thomas, D. D., and L. Stryer. 1982. Transverse location of the retinal chromophore of rhodopsin in rod outer segment disk membranes. *J. Mol. Biol.* 154:145–157.
10. Gennis, R. B., and C. R. Cantor. 1972. Use of nonspecific dye labeling for singlet energy-transfer measurements in complex systems. A simple model. *Biochemistry.* 11:2509–2517.
11. Gennis, L. S., R. B. Gennis, and C. R. Cantor. 1972. Singlet energy-transfer studies on associating protein systems. Distance measurements on trypsin, α-chymotrypsin, and their protein inhibitors. *Biochemistry.* 11:2517–2524.
12. Rehorek, M., N. A. Dencher, and M. P. Heyn. 1982. Fluorescence energy transfer from diphenylhexatriene to bacteriorhodopsin in lipid vesicles. *Hoppe-Seyler's Z. Physiol. Chem.* 363:546–547.
13. Struck, D. K., D. Hoekstra, and R. E. Pagano. 1981. Use of resonance energy transfer to monitor membrane fusion. *Biochemistry.* 20:4093–4099.
14. Gingold, M. P., J.-L. Rigaud, and Ph. Champeil. 1981. Fluorescence energy transfer between ATPase monomers in sarcoplasmic reticulum reconstituted vesicles. *Biochimie (Paris).* 63:923–925.
15. Dewey, T. G., and G. G. Hammes. 1980. Calculation of fluorescence energy transfer on surfaces. *Biophys. J.* 32:1023–1035.
16. Eisinger, J., W. E. Blumberg, and R. E. Dale. 1981. Orientational effects in intra- and intermolecular long range excitation transfer. *Ann. NY Acad. Sci.* 366:155–175.
17. Estep, T. N., and T. E. Thompson. 1979. Energy transfer in lipid bilayers. *Biophys. J.* 26:195–207.
18. Wolber, P. K., and B. S. Hudson. 1979. An analytic solution to the Förster energy transfer problem in two dimensions. *Biophys. J.* 28:197–210.
19. Snyder, B., and E. Freire. 1982. Fluorescence energy transfer in two dimensions. A numeric solution for random and nonrandom distributions. *Biophys. J.* 40:137–148.
20. Dale, R. E., J. Novros, S. Roth, M. Edidin, and L. Brand. 1981. Application of Förster long-range excitation energy transfer to the determination of distributions of fluorescently-labeled concanavalin-A receptor complexes at the surfaces of yeast and of normal and malignant fibroblasts. *In* Fluorescent Probes. G. S. Beddard and M. A. West, editors. Academic Press Inc. Ltd., London. 159–181.
21. Fernandez, S. M., and R. D. Berlin. 1976. Cell surface distribution of lectin receptors determined by resonance energy transfer. *Nature (Lond.)* 264:411–415.
22. Chan, S. S., D. J. Arndt-Jovin, and T. M. Jovin. 1979. Proximity of lectin receptors on the cell surface measured by fluorescence energy transfer in a flow system. *J. Histochem. Cytochem.* 27:56–64.
23. Jovin, T. M., and D. J. Arndt-Jovin. 1982. Flow sorting on the basis of morphology and topology. *In* Trends in Photobiology. C. Helene, M. Charlier, Th. Montenay-Garestier, and G. Laustriat, editors. Plenum Publishing Corp., New York. 51–66.
24. Jovin, T. M. 1979. Fluorescence polarization and energy transfer: theory and application. *In* Flow Cytometry and Sorting. M. R. Melamed, P. F. Mullaney, M. L. Mendelsohn, editors. John Wiley & Sons, Inc, New York. 137–165.
25. Holtkamp, B., K. F. Lindahl, M. Segall, and K. Rajewsky. 1979. Spontaneous loss and subsequent stimulation of H-2 expression in

clones of a heterozygous lymphoma cell line. *Immunogenetics.* 9:405–421.

26. De Petris, S. 1978. Immunoelectron microscopy and immunofluorescence in membrane biology. Methods Membr. Biol. 9:1–201.
27. Arndt-Jovin, D. J., B. G. Grimwade, and T. M. Jovin. 1980. A dual laser flow sorter utilising a CW pumped dye laser. *Cytometry.* 1:127–131.
28. Szöllősi, J., L. Trón, S. Damjanovich, S. H. Helliwell, D. J. Arndt-Jovin, and T. M. Jovin. 1984. Fluorescence energy transfer measurements on cell surfaces. A critical comparison of steady-state fluorimetric and flow cytometric methods. *Cytometry.* In press.
29. Hardman, K. D., M. K. Wood, M. Schiffer, A. B. Edmundson, and C. F. Ainsworth. 1971. Structure of concanavalin A at 4.25 Å resolution. *Proc. Natl. Acad. Sci. USA.* 68:1393–1397.
30. Quiocho, F. A., G. N. Reeke, J. W. Becker, W. N. Limpscomb, and G. M. Edelman. 1971. Structure of concanavalin A at 4 Å resolution. *Proc. Natl. Acad. Sci. USA.* 68:1853–1857.
31. Damjanovich, S., L. Tròn, J. Szöllősi, R. Zidovetzki, W. L. C. Vaz, F. Regateiro, D. J. Arndt-Jovin, and T. M. Jovin. 1983. Distribution and mobility of murine histocompatibility H-2K^k antigen in the cytoplasmic membrane. *Proc. Natl. Acad. Sci. USA.* 80:5985–5989.
32. Zidovetzki, R., Y. Yarden, J. Schlessinger, and T. M. Jovin. 1981. Rotational diffusion of epidermal growth factor complexed to cell surface receptors reflects rapid microaggregation and endocytosis of occupied receptors. *Proc. Natl. Acad. Sci. USA.* 78:6981–6985.
33. Hamori, E., D. J. Arndt-Jovin, B. G. Grimwade, and T. M. Jovin. 1980. Selection of viable cells with known DNA content. *Cytometry.* 1:132–135.